
Predicting Cervix Types with Convolutional Neural Networks

Lan-Anh Ngo-Quy

Dina Ginzburg

Swarthmore College,
500 College Ave,
Swarthmore, PA, 19081

LNGOQUY1@SWARTHMORE.EDU

DGINZBU1@SWARTHMORE.EDU

Abstract

Cervical cancer is easily treatable when detected in its pre-cancerous stage. Many women, particularly those who are low-income, benefit from programs which identify and treat cervical cancer within a single visit. Depending on their cervix type, further treatment may be required for the patient. This decision is very important, and since identifying the transformation zones is not an easy task for healthcare providers, developing an algorithm to correctly identify cervix type based on cervical images is critical, especially for related research dealing with large datasets. In this paper we will present our solution to predicting the cervix types. First, we segmented ROI to exclude irrelevant information while preserving the cervix in its entirety. The processed images were then split into training, tuning and test sets and fed into a Convolutional Neural Network (CNN). We also implemented the Bag of Words method and a Multi-Layer Perceptron, to compare our CNN's performance to other classifiers. We found that Bag of Words performed the best with accuracy rate of 56.78%, while CNN reaches an accuracy rate of 54.4%, which although significantly better than chance and better than average performance of the 3 methods (51.85%), is not accurate enough for our classifier to be reliable. Further work to boost the classifier's performance would be better data augmentation, image segmentation methods that match the cervix boundary more closely and implementing fine-tuning with weights from a pre-trained CNN.



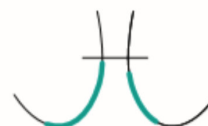
Type 1

- Completely ectocervical
- Fully visible
- Small or large



Type 2

- Has endocervical component
- Fully visible
- May have ectocervical component which may be small or large



Type 3

- Has endocervical component
- Is not fully visible
- May have ectocervical component which may be small or large



Figure 1. Three types of cervix.

1. Introduction

Treatment for cervical cancer is relatively simple when it is detected in a pre-cancerous stage. However, many health care specialists lack the expertise to determine the appropriate method of treatment— which can vary wildly based on each patient's unique physiology. Applying the wrong treatment can not only increase health risks for the patient, but is also very costly. MobileODT, a company which seeks to prevent cervical cancer by developing and selling the Enhanced Visual Assessment (EVA) System. The EVA system is a digital toolkit for health care workers, which includes a mobile-phone based medical device designed to use biomedical optics to screen and treat patients for cervical cancer (Intel, 2017). MobileODT and Intel have de-

cided to partner in a Kaggle competition with the purpose of developing an algorithm which accurately predicts a patients cervix type based on cervix images. We tried three different approaches to solving this problem: a CNN, Bag of Words, and a Multi-Layer Perceptron. We found that we were able to get Bag of Words to perform the best, although all three methods had lackluster results.

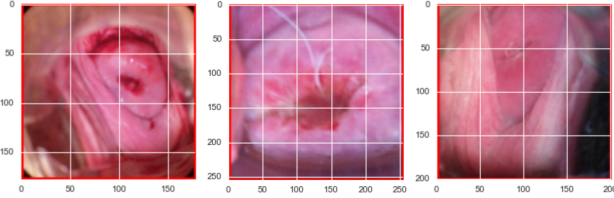


Figure 2. Cervigrams from left to right: type 1, type 2, type 3.

Most Cervical cancers begin in the cells of the transformation zone (an area of the cervix). There are three cervix types and each one has a different transformation zone location. It is important to know what the cervix type is because cervix types 2 and 3 might include hidden lesions and require different treatment. However the transformation zones aren't always visible and they're difficult to identify for health care providers, so an algorithm-based approach can greatly aid real-time determinations about patient treatment (Intel, 2017). Fig. (2) shows an example for each type of cervix in the dataset.

We decided to try a combination of image preprocessing and a Convolutional Neural Network (CNN) to classify the cervix images. We used segmentation on the data to get the Region of Interest for each image, and eliminated white noise. We used a combination of methods outlined by Greenspan and a kaggle kernel authored by the user "chattob". We then fed the data into a CNN, experimenting with different types of layers and hyperparameters. We drew on Srivastava's work on Dropout layers and Ioffe's work on Batch Normalization to reduce overfitting in our CNN. We also implemented Bag of Words and a Multi-Layer Perceptron, and compared accuracy rates among these three methods.

We were surprised to find that despite tinkering with hyperparameters and running multiple tests with different architectures, our Convolutional Neural Network only performed better than the Multi-Layer Perceptron. In fact, Bag of Words had the highest accuracy of all three methods we implemented. However, none of the three methods were able to get exceptionally high accuracy on the test set, with Bag of Words reaching only 56.78% accuracy.

2. Methods

Our algorithm for cervix prediction consists of image preprocessing to find the Region of Interest in each image and reduce noise in the image. The processed data is then fed into a Convolutional Neural Network. To compare the performance of our implementation of the CNN, we also implemented the Bag of Visual Words (BoW) method and a Multi-layer Perceptron (MLP).

2.1. Image Preprocessing

Before the images can be fed into any classifying algorithm, they need to go through a preprocessing step which will produce smaller sub-images containing only the cervix area, our Region of Interest (ROI). Challenges in identifying the correct region include lack of distinct boundaries among different tissues, the small color range, reflection artifacts, large variability in the viewing angles, cervix sizes and tissue types presented in the images. A summary of the image segmentation process is illustrated by Fig. (3). To exclude the black circular frames often seen in the cervigrams, our method cropped the circle out by finding the maximum continuous rectangle area. Since the cervix region has a relatively pink color and should be at the center of the cervigram, in function `Ra.space` we chose to represent each pixel of the image by 2 values: the minimum of the a color of the Lab color space $a = 150$ and the pixels red channel value, and the pixels distance R from the image center. Each image is then separated into 2 clusters using Gaussian Mixture Model in 2-dimensional space. The ROI will then be the largest connected component among the pixels belonging to the cluster with the highest a and the lowest R values (chattob, 2017).

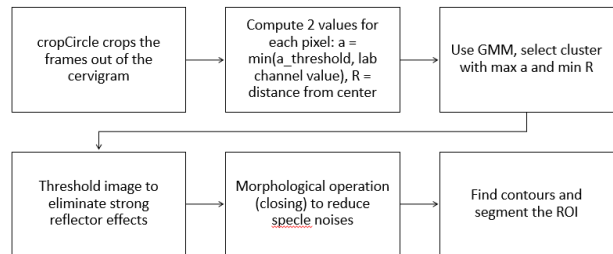


Figure 3. Segmentation algorithm.

To make the image less noisy, pixels in small and bright discontinuous regions (SR) caused by strong reflectors on the cervix surface are detected by thresholding. We created a thresholded mask and removed those areas which were above the threshold by setting them equal to (0, 0, 0). This prevents these areas from interfering with the content analysis of the surrounding regions. Additionally, Morphologi-

cal operation closing was used to remove speckle noises. Our final preprocessing step was to find contours which we then use to choose our width and height for our ROI (Hayit Greenspan, 2009).

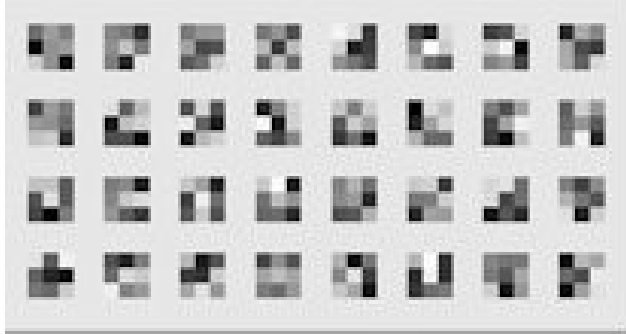


Figure 4. Kernels for the first Convolutional Layer of our CNN architectures.

2.2. Convolutional Neural Networks

Convolutional Neural Networks are very similar to regular Neural Networks: they are made up of neurons with weights and biases, which take a set of inputs and perform a dot product. However, CNNs make the explicit assumption that the inputs are images. This allows for a more efficient forward function and reduces the number of parameters in the network. In a regular Neural Network, each neuron is fully connected to each neuron in the previous layer. This does not scale well to images, where each fully connected neuron would require $\text{width} \times \text{height} \times 3$ weights. CNNs solve this problem by constraining the architecture - each layer of the network arranges its neurons three-dimensionally by width, height, and depth. Neurons in each layer are only connected to a small patch of the previous layer. For our project, we used the Keras neural network library (Karpathy, 2017).

Our CNN used three built-in Keras layers: a Convolution layer (Conv), a Pooling layer (Pooling), and a Fully-Connected layer (FC). The Convolution layer is the main component of a CNN, doing most of the heavy computational work. Each parameter in this layer is a learnable filter (with height and width much smaller than the input image) which is convolved along the width and height of the image during the forward pass. This process produces a 2-dimensional activation map which gives the filter response at each position in the image. The network will learn filters that activate when they see certain features in the image. Fig. (4) shows the kernels for the first convolutional layer of our best-performing CNN model. The Pooling layer is inserted after a Convolution layer in order to reduce the size of the representation. This results

in not only a reduced number of parameters and computation time, but also helps to prevent overfitting. The final Fully-Connected layer functions just like a regular fully-connected Neural Network. These layers can be arranged in any order, sometimes with many layers of Convolution and Pooling. (Karpathy, 2017). Fig. (5) demonstrates an example arrangement of the layers in a CNN.

Additional layers used our architecture were BatchNormalization and Dropout layers. In deep neural networks, the changes in parameters of the previous layers will result in a different distribution of each layers input. This requires lower learning rates and careful initialization, slowing down the training (Sergey Ioffe, 2015). A method to address this problem is normalizing layer inputs, thus following common practice (Karpathy, 2017), we inserted a Batch Normalization layer immediately after our convolutional layer. The Dropout layer prevents overfitting during training by randomly dropping units along with their connections from the neural network (Nitish Srivastava, 2014). In the tests conducted, we added a Dropout layer after the convolutional layer and the BatchNormalization layer.

2.2.1. PARAMETERS FOR CNNs

Convolutional Neural Networks require that we provide certain parameters. For the Convolutional layer, W is the input volume - or the size ($\text{width} \times \text{height} \times \text{depth}$) of the image. F is the receptive field size - or the size of the filter in the Convolution layer. S is stride - or how many pixels we move the filter each time we slide it across the image. Sometimes it is convenient to pad the input volume with zeros around the border - the size of this border is P . These variables will be referenced later in this paper (Karpathy, 2017).

2.3. Bag of Words

To compare our CNN performance to other methods, we also implemented Bag of Words (BOWs) for images, fig. (6) illustrates the steps taken in this algorithm. BOWs works by treating each image as a document and each image feature as a word. Once features are detected (by sliding a kernel along the images), they are represented by vectors called feature descriptors. BOWs functions by creating a codebook which converts these vectors into codewords, which can be representative of multiple vectors. To create the codebook, we used K-means clustering on the vectors, and chose the centers of each cluster as the codeword. An image is then represented by the histogram of the codewords, which allows us to classify the image based on its histogram using a multi-class AdaBoost classifier from sklearn (Tsai, 2012).

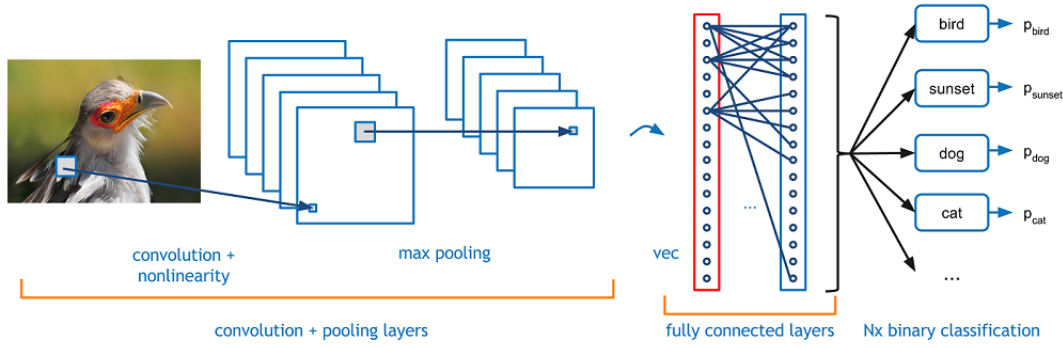


Figure 5. A Convolutional Neural Network with Convolution, Pooling, and Fully Connected layers.

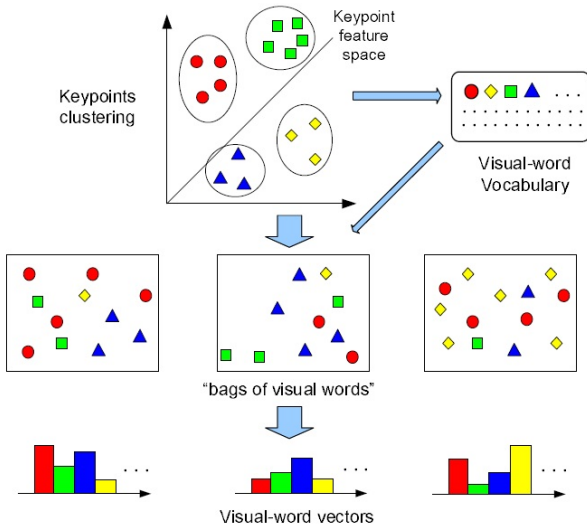


Figure 6. Bag of Words algorithm.

2.4. Multi-Layer Perceptron

The other method we implemented to compare our CNN performance to was the Multi-Layer Perceptron (MLP). An MLP is an artificial neural network with multiple layers of nodes. Each layer is fully connected to the next one. Our implementation used a single hidden layer with 16 hidden nodes.

3. Experiments

We used the datasets downloaded from kaggle's Intel & MobileODT Cervical Cancer Screening <https://www.kaggle.com/c/intel-mobileodt-cervical-cancer-screening>. The datasets consist of 250 images labeled Type 1, 781 images labeled Type 2, and 450 im-

ages labeled Type 3. Most of the images contain irrelevant details to our training algorithm such as medical devices and unidentifiable tissue, so we used the method specified by Greenspan et. al. (Hayit Greenspan, 2009) to segment the cervix as smaller sub-images containing only the region of interest (ROI). The images after segmentation had different dimensions, so we chose the minimum dimension (58x58) to resize all of them. The final preprocessing step was converting the data type to float32 and normalizing the data to the range of [0, 1].

Even though the segmentation method correctly identified the ROI for most of the images, there are some images that still have parts of medical devices. The sizes vary a lot among the images (the largest size after segmentation is 256, but all images are then scaled to 58x58 - the minimum shape detected). Fig. (7) shows an example of two images: the one on the left is properly segmented, while the one on the right is an example of poor segmentation.

Since only the labels for the training set are provided, for supervised learning we used cross validation. We first split the images into train and test sets by a ratio of 2:1. To choose the best set of hyperparameters we further split X_train into a training set and tuning set by a ratio of 4:1. Thus, the final training, tuning, and test sets consist of 793, 199 and 489 images. For feeding X_train and Y_train into the CNN, we needed to convert our 1-dimensional label arrays Y_train and Y_test into 3-dimensional label matrices.

To understand our CNN net better, we conducted several timed tests to figure out what should be the best set of hyperparameters. For the images of size 58 x 58, we chose to set the receptive field size $F = 3$, with stride $S = 0$ and padding on the border of the images $B = 1$. The choice of a small receptive field size and 0 stride is to avoid losing too much information. The size of the kernel for MaxPooling layer was set to (2,2) since any larger number would demand K to be larger in the previous convolutional layer(s),

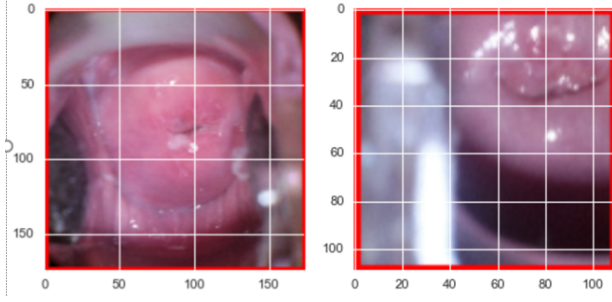


Figure 7. Two examples of image segmentation. Left example worked correctly, while right example failed.

which would make the model prone to overfitting to the training data. All of the layers we used in the testing architectures used 'relu' activation except for the last FC layer when softmax was used instead. We adjusted the number(s) of kernels K for the convolutional layer, the number of output nodes for the FC layer, changed the batch size, and rearranged the architecture of the neural networks. For the FC before the last one, we used weight regularization to further prevent overfitting. We run all the testing architectures with batch size of 10 in 8 epochs, unless specified otherwise. Our model's architectures for testing is summarized by Table. (1).

In our comparison test with MLP, Y_{train} and Y_{test} were kept in the original shape of 1-dimensional array, while X_{test} and X_{train} needed reshaping into 2-dimensional matrices. We transformed X_{train} using only its row vectors, from (793, 58, 58, 3) into a (793, 10092) matrix, and similarly for X_{test} . For BOWs with the input as an array of grayscale images (793, 58, 58), we detected the features by extracting 5x5 patches from each image. This resulted in an array of size (793, 54, 54, 5, 5) which we then reshaped into a (793*53*53, 5*5) 2-dimensional array. Thus each image is represented by 53*53 feature descriptors. These feature descriptors were then used to compute the histogram by using the codebook. The resulting histograms served as our training features for the model. Similarly for the test set, we detected 5x5 patches for each image and computing their histograms with the same codebook. Fig. (9) and Fig. (10) show the cluster assignment of patches and the histogram according to our produced codebook for an example image.

4. Discussion

Tests 1 through 3 (Table 2.) had the same architecture implementation except for variation in the number of kernels for the convolutional layer and the output size of the FC layer. All three tests resulted in the same score on the tun-

Table 1. Summary of the CNN architectures used for testing

ARCHITECTURE	LAYERS
CNN0	CONV LAYER(K) → POOLING → BATCHNORMALIZATION → FLATTEN → FC(D) → BATCHNORMALIZATION → FC(SOFTMAX, 3)
CNN1	CONV LAYER(K) → POOLING → BATCHNORMALIZATION → DROPOUT(0.25) → FLATTEN → FC(D) → BATCHNORMALIZATION → DROPOUT(0.25) → FC(SOFTMAX, 3)
CNN2	CONV LAYER(K) → POOLING → BATCHNORMALIZATION → DROPOUT(0.25) → CONV LAYER(16) → POOLING → BATCHNORMALIZATION → FLATTEN → FC(D) → BATCHNORMALIZATION → DROPOUT(0.25) → FC(SOFTMAX, 3)
CNN3	CONV LAYER(K) → POOLING → BATCHNORMALIZATION → DROPOUT(0.25) → CONV LAYER(16) POOLING → BATCHNORMALIZATION → CONV LAYER(8) → POOLING → BATCHNORMALIZATION → FLATTEN → FC(D) → BATCHNORMALIZATION → DROPOUT(0.25) → FC(SOFTMAX, 3)
CNN4	SAME AS CNN1 BUT WITHOUT BATCHNORMALIZATION LAYER
BOWs	KERNEL SIZE = (5, 5), NCLUSTERS = 50
MLP	SINGLE HIDDEN LAYER SIZE 16

ing set, which was higher than the score on training set in all cases. This indicates that increasing the number of layers or output size of FC did not increase the performance of our model.

With the same number of kernels for convolutional layer and output size of FC layer, with a Dropout Layer added to the architecture, test 4 gave the same max accuracy as test 3, however scores better on the tune set, and in fact this is the best score we got across all the tests on the tuning set.

From test 4 to test 5, we increased the complexity of our model with architecture CNN2 (Table 1.) by adding another Convolutional Layer with $K=16$. This led to a decrease in the tuning score, the resulting accuracy rate scored on the training and tuning sets in tests 4 and 5 is shown by fig. (8). With the same architecture of 2 Convolutional layers,

Predicting Cervix Types with Convolutional Neural Networks

Table 2. Results of testing architectures on the training and tuning sets. Best result is highlighted in bold.

NUMBER	CNN ARCHITECTURE	K	FULLY CONNECTED OUTPUT SIZE	TRAIN SCORE	TUNE SCORE	FIT TIME
1	CNN0	16	8	.5233	.5377	11.2947
2	CNN0	16	16	.5246	.5377	11.6939
3	CNN0	32	8	.5158	.5377	32.6779
4	CNN1	32	8	.5158	.5427	40.3847
5	CNN2	32	8	.5158	.5377	60.9466
6	CNN2	16	8	.5259	.4874	33.9327
7	CNN3	32	8	.5158	.4221	97.2797
8	CNN3	64	8	.5032	.5327	142.4461
9	CNN1 (BATCH SIZE =10)	32	8	.5158	.5377	25.4096
10	CNN1 (BATCH SIZE =32)	32	8	.5158	.5377	24.8567
11	CNN4	32	8	.5158	.5377	32.053
12	CNN1 (WITHOUT BATCHNORMALIZATION LAYER)	32	8	.5158	.5377	35.8653
13	CNN1 (F =5)	32	8	.5158	.5377	36.4211

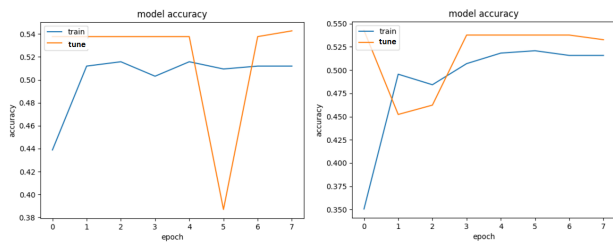


Figure 8. Accuracy for training and tuning sets on test 4 (left) and test 5 (right).

comparing test 5 and test 6 shows that with fewer layers, our model performed worse on the tuning set and seemed to overfit the dataset with a higher score on the training set. Similarly, with another Convolutional layer added in CNN3, comparing test 7 with 5 shows worse performance on the tuning set and overfitting with higher train score. However, test 8 indicates that an increase in the number of kernels in the first Convolutional layer gave better accuracy rate on the tuning set. From our results in Table (2) and the

graphs in Figure (10), we can see that applying the model to the tuning set often outperforms the training set, so we conducted test 10 and 11 with a smaller number of epochs (5) and increased the batch size in test 10 (32). However, results show equivalent accuracy rates on both train and tuning sets.

Table 3. Results on the training and test sets for CNN, BOWs and MLP

METHOD	TRAIN SCORE	TUNE SCORE	TIME
CNN	0.5183	0.5440	9.6548
BOWs	0.5813	0.5678	2.8761
MLP	0.9130	0.4438	1.4576

Choosing the best performance seen in test 4, we conducted test 12: an architecture set up exactly the same as in test 4 except without the BatchNormalization layer. Even though the scores on the training set are the same, with BatchNor-

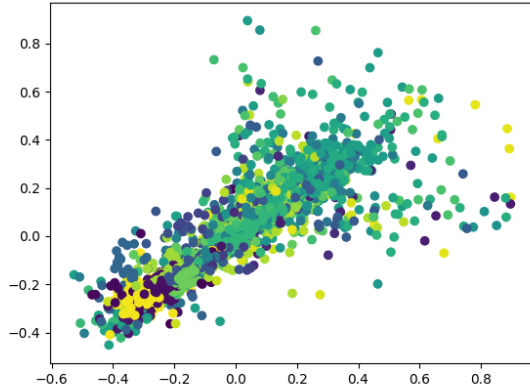


Figure 9. Cluster assignment of patches for img7 (type 1) using the codebook.

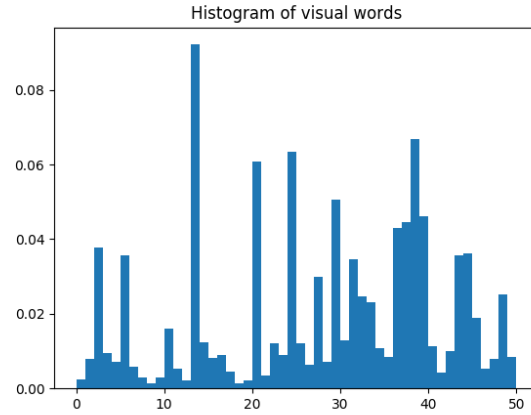


Figure 10. Histogram of patches for img7 (type 1) using the codebook.

malization test 4 performed better on the tuning set. Observing the kernel weights of the convolutional layer in Fig. (4), we conducted an additional test 13 with CNN1 architecture but increased receptive field size $F = 5$ to see if a bigger kernel can extract more useful features of the images. This resulted in a similar score on the training set but a lower score on the tuning set (.5377 versus .5427).

We implemented CNN1 with batch size=10, epoch=8 on the test set and yielded an accuracy rate=.5440, close to our score on the tuning set (.5427) in 39.8926s fitting time. Comparing with other 2 methods, BOWs gained a better accuracy rate (.5678) on the test set, while MLP gave a lower score of (.4438). Both BOWs and MLP produced a better score on the training set, especially MLP (training accuracy = .9130), suggesting that the classifiers overfitted. In comparison with the average accuracy rate on the test set among all three classifiers (.5185) our CNN gives a score better than average (even though the score is only 64.26% better than chance (.3333)). Fitting time-wise, the method BOWs gives a better performance with better score than CNN (39.8926 versus 2.8761), however the process of computing the histogram from the codebook took a lot of waiting time.

Through tweaking with the choice of number of layers, size of layers and choice of hyperparameters, we observed in our experiments that the increase in number of layers, especially convolutional layer, and increase in number of layer's output size increased the fitting time.

5. Conclusion

By conducting multiple tests varying the architecture of the model and the hyperparameters for the CNN, we found that the model performed best on the tuning set with CNN1. Even though the rate obtained on the testing set (.5440) is only 63.21% better than chance, comparing with other methods we tried, CNN performed better than average (.5185). The best performance across CNN, BOWs and MLP is BOWs with a codebook constructed by segmenting 5x5 patches from each image and using k-means to determine 50 cluster centers (accuracy rate = .5678). However, this method demands a lot of time for computing the histograms for each image to build the training set.

While further engineering the CNN by adjusting the number of layers, layer output sizes and other hyperparameters can help increase the accuracy rate, data augmentation is also important. The image processing algorithm could work better by eliminating similar images in our dataset. Another step is to refine the initial ROI such that it matches the cervix boundary more closely. This could be done by using prior shape information, combining feature values measured along the shape boundary such as edges. While our current segmentation algorithm zeroed out the regions affected by strong reflectors already, a better next step would be to propagate surrounding pixels into specular regions, creating smooth filling of the image (Hayit Greenspan, 2009).

Further work to boost the performance of the classifier is trying out the fine-tuning approach. Knowing that a pre-trained CNN model have already learned features relevant to our classification problem such as edges, regional features, we can improve our model by taking advantage of the

pre-trained models resulting weights. An implementation of this would be instantiating the convolutional base with the weights of a pre-trained CNN such as VGG16 (Karen Simonyan, 2014), freezing all the layer of VGG16 up to the last convolutional block, then add our previously defined FC model on top (keras blog).

References

- chattob. Cervix segmentation (gmm), 2017. URL <https://www.kaggle.com/chattob/intel-mobileodt-cervical-cancer-screening/cervix-segmentation-gmm>.
- Hayit Greenspan, et. al. Automatic detection of anatomical landmarks in uterine cervix images. *IEEE Transactions on Medical Imaging*, 2009.
- Intel. Intel & mobileodt cervical cancer screening, 2017. URL <https://www.kaggle.com/c/intel-mobileodt-cervical-cancer-screening>.
- Karen Simonyan, et. al. *ICLR 2015*, 2014.
- Karpathy, Andrej. Convolutional neural networks for visual recognition, 2017. URL <http://cs231n.github.io/convolutional-networks>.
- Nitish Srivastava, et. al. Dropout: A simple way to prevent neural networks from overfitting. *Journal of Machine Learning Research*, 2014.
- Sergey Ioffe, Christian Szegedy. Batch normalization: Accelerating deep network training by reducing internal covariate shift, 2015.
- Tsai, Chih-Fong. Bag-of-words representation in image annotation: A review. *International Scholarly Research Network*, 2012.